

Systematic analysis of expression profiles and prognostic significance of the FGF gene family in pancreatic adenocarcinoma

YU-XIN CHEN^{1,2*}, XIAO-JUAN LIU^{1,2*}, LING YANG^{1,2}, JIA-JING HE^{1,2}, YONG-MEI JIANG^{1,2} and JIA MAI^{1,2}

¹Department of Laboratory Medicine, West China Second University Hospital, Sichuan University;

²Key Laboratory of Birth Defects and Related Diseases of Women and Children, Sichuan University, Ministry of Education, Chengdu, Sichuan 610041, P.R. China

Received May 9, 2022; Accepted September 16, 2022

DOI: 10.3892/ol.2022.13555

Abstract. Pancreatic adenocarcinoma (PAAD) is a malignant tumor with one of the highest associated mortality rates worldwide, and a 5-year survival rate of <5%. Fibroblast growth factors (FGFs) serve important roles in numerous cellular functions, and dysregulation of FGFs contributes to various cancer types. However, there are few reports on the function of FGFs in PAAD. The Assistant for Clinical Bioinformatics database, Gene Expression Profiling Interactive Analysis, Kaplan-Meier plotter and Tumor Immune Estimation Resource were utilized to perform the protein-protein interaction network, functional enrichment, univariate Cox regression, least absolute shrinkage and selection operator (LASSO) Cox, differential expression, prognostic value and immune cell infiltration analyses of FGFs in patients with PAAD. Immunohistochemistry (IHC) was used to verify the predictive value of the model. A total of 22 FGF genes were identified. Based on the results of LASSO Cox regression analysis, a total of six genes, including FGF2, FGF8, FGF9, FGF13, FGF17 and FGF22, were selected for the establishment of the prognostic gene signature. High transcriptional levels of FGF17 and FGF22 were significantly associated with long overall survival. The expression of FGFs was associated with the infiltration of various immune cells. According to univariate and multivariate analyses, FGF2 and FGF8 may be useful independent prognostic biomarkers for the prognosis of patients with PAAD. IHC demonstrated that FGF2 and FGF8 were more highly expressed in PAAD tissues

compared with that in normal tissues. The present findings offer a novel understanding for the selection of FGF prognostic biomarkers in PAAD.

Introduction

Pancreatic adenocarcinoma (PAAD), which is expected to become the second leading cause of cancer-associated mortality worldwide, is usually lethal despite treatment efforts (1). Furthermore, ~80% of patients exhibit advanced cases at diagnosis due to the lack of specific tumor markers and undefined early symptoms (2). Limited and delayed diagnostic strategies increase the difficulty of diagnosis, thus severely impeding various therapeutic options. Although increasing evidence suggests that pancreatic cancer is linked to several variables, such as smoking, alcohol consumption, coffee intake, a high-fat and protein diet, and genetic background (3-5), the causes of pancreatic cancer remain unknown.

At present, treatment options for PAAD focus mostly on the clinicopathological evaluation of the malignancy, and include surgery followed by chemotherapy and radiotherapy (6,7). According to sequencing data, pancreatic cancer comprises markedly diverse tumors that acquire resistance to standard chemotherapy and radiation therapy (8,9). As a result, traditional chemotherapy and radiotherapy often fail to produce the anticipated therapeutic impact, while gemcitabine-targeted treatment fails to increase overall survival (OS). Therefore, the identification of novel effective biomarkers for early diagnosis and prognosis is required to improve the survival rate of patients with PAAD.

In recent years, emerging data have demonstrated that essential genes and signaling pathways, including KRAS, p53, SMAD4, Wnt, PI3K/AKT and Notch signaling, are critical in the tumorigenesis and progression of PAAD (10,11). However, at present, there is no effective clinical treatment for PAAD that targets these genes and signaling pathways. Novel therapies to prevent pancreatic cancer growth and metastasis are urgently required. It has been reported that numerous growth factor signaling pathways are involved in PAAD tumorigenesis and progression, and fibroblast growth factors (FGFs) signaling pathways are an example of this (12,13). FGFs are a large family of >20 members that encode secreted polypeptides and act through tyrosine kinase receptors known as FGF

Correspondence to: Dr Yong-Mei Jiang or Dr Jia Mai, Department of Laboratory Medicine, West China Second University Hospital, Sichuan University, 20 Ren Min Nan Lu, Section 3, Chengdu, Sichuan 610041, P.R. China
E-mail: jiang_ym@scu.edu.cn
E-mail: maijia@mail2.sysu.edu.cn

*Contributed equally

Key words: pancreatic adenocarcinoma, fibroblast growth factors, fibroblast growth factor 2, fibroblast growth factor 8, prognosis, biomarkers

receptors (14). FGF is named for its promotion of fibroblast proliferation, and is present in various tissues (15). FGFs are involved in various cellular activities, including cell proliferation, metabolism, differentiation and tissue repair (16). It has been reported that FGFs participate in cancer progression in multiple types of tumor, and are closely associated with prognosis. Bock *et al* (17) found that FGF2 could be released by cancer cells to enable apoptotic resistance upon apoptotic stress, while an association existed among increased FGF signaling, anti-apoptotic Bcl-2 protein expression and poor patient prognosis. Additionally, FGF18 promotes the tumor proliferation and metastasis of non-small cell lung cancer (NSCLC) via the histone deacetylase 7- β -catenin-FGF18 pathway (18). However, high FGF9 expression is associated with good prognosis in ovarian cancer (19). Cancer types that are triggered by FGF signaling can be treated with targeted medicines such as tyrosine kinase inhibitors (20). Targeting FGF signaling is a realistic therapeutic strategy, as evidenced by the fact that treatments are currently being utilized in several patient populations (21-23). Furthermore, previous studies have demonstrated that FGFs participate in the development of chemoresistance in tumor cells (24). However, the role and mechanism of FGFs in PAAD are unclear. Therefore, the present study aimed to further explore the role and potential mechanism of FGFs in PAAD.

In the present study, the prognostic value of the FGF gene family in PAAD was comprehensively analyzed using RNA-seq data and clinical information from public databases, and a risk score was constructed. It was revealed that FGF2 and FGF8 may be useful independent prognostic biomarkers for the prognosis of patients with PAAD. Immunohistochemistry (IHC) also validated that FGF2 and FGF8 were more highly expressed in PAAD tissues compared with that in normal tissues. The present findings may offer a novel understanding of the selection of prognostic biomarkers of FGFs in PAAD.

Materials and methods

Data acquisition and processing. mRNA expression datasets and corresponding clinical information of The Cancer Genome Atlas (TCGA)-PAAD were obtained from the Gene Expression Profiling Interactive Analysis (GEPIA) database (<http://gepia.cancer-pku.cn/>). Data were analyzed using R (version 4.0.3) (<https://www.r-project.org/>) and the matched version of R Bioconductor package (<http://bioconductor.org/>). The Assistant for Clinical Bioinformatics database (<https://www.aclbi.com/static/index.html#/>) was used for cluster analysis and construction of the risk assessment model for FGFs of the PAAD dataset. These data are open resources, and thus, ethics approval or informed patient consent were not required for the use of these data in the current study.

Protein-protein interaction (PPI) network construction. A PPI network was constructed using the Search Tool for the Retrieval of Interacting Genes/Proteins database (version 11.5) (<https://cn.string-db.org/>). FGFs, including FGF1, FGF2, FGF3, FGF4, FGF5, FGF6, FGF7, FGF8, FGF9, FGF10, FGF11, FGF12, FGF13, FGF14, FGF16, FGF17, FGF18, FGF19, FGF20, FGF21, FGF22 and FGF23, were placed in the search box. The minimum required interaction score was

set at 0.4, and active interaction sources included text mining, experiments, databases, co-expression, neighborhood, gene fusion and co-occurrence.

Correlation analysis. RNA-sequencing expression profiles and corresponding clinical information for TCGA-PAAD were downloaded from TCGA dataset (<https://portal.gdc.com>). The two-gene correlation map is realized by the R software package ggstatsplot, and the multi-gene correlation heatmap is displayed by the R software package. Spearman's correlation analysis was used to describe the correlation between quantitative variables without a normal distribution. $P < 0.05$ was considered to indicate a statistically significant difference and correlation coefficients with an absolute value of > 0.3 were considered to show a correlation. All these analyses were performed with a web tool called ASSISTANT for Clinical Bioinformatics that combines all these functions (https://www.aclbi.com/static/index.html#advance_prognosis).

Functional and pathway enrichment analysis. Gene Ontology (GO) (<http://geneontology.org/>) analysis was performed to determine the potential biological functions of the FGF gene family using the clusterProfiler R package (version 4.4.4; <https://bioconductor.org/packages/release/bioc/html/clusterProfiler.html>). GO analysis was performed according to a threshold of $P < 0.05$ and $q < 1$.

Identification of molecular subtypes. Cluster analysis of 20 FGF family genes in pancreatic cancer was performed. Raw counts of RNA-sequencing data and corresponding clinical information were obtained from TCGA. ConsensusClusterPlus (version 1.60.0) was used for consistency analysis. The maximum number of clusters was 6, and 80% of the total sample was drawn 100 times. Pheatmap package (version 1.0.12) was used to generate clustering heatmaps. Prognostic differences were analyzed among different subgroups (groups C1, C2 and C3), and the survivalROC package was utilized to draw the survival curve. All these analyses were performed with a web tool called ASSISTANT for Clinical Bioinformatics that combines all these functions (https://www.aclbi.com/static/index.html#advance_prognosis).

Construction of a risk assessment model. The least absolute shrinkage and selection operator (LASSO) regression algorithm were used for feature selection, using 10-fold cross-validation, in the R software package glmnet (version 4.1-1). Kaplan-Meier plotter survival analysis with the log-rank test was also used to compare the survival difference between the low-risk and high-risk groups. timeROC (v 0.4) analysis was performed to compare the predictive accuracy of each gene and risk score. All these analyses were performed with a web tool called ASSISTANT for Clinical Bioinformatics that combines all these functions (https://www.aclbi.com/static/index.html#advance_prognosis).

Survival prognosis analysis. GEPIA 2 (<http://gepia2.cancer-pku.cn/>) was used to obtain the OS significance map data of FGFs in TCGA-PAAD. Cut-off-high (50%) and cut-off-low (50%) values were used as the expression thresholds for dividing the high- and low-expression cohorts.

Unpaired Student's t-test was performed for data analysis. $P < 0.05$ was considered to indicate a statistically significant difference.

Immune infiltration analysis. The 'Immune-Gene' module of Tumor Immune Estimation Resource (TIMER; <http://timer.cistrome.org/>) was used to explore the associations among FGF2, FGF8, FGF9, FGF13, FGF17 and FGF22 expression, and immune infiltrates across TCGA-PAAD. Immune CD8⁺ T cells, CD4⁺ T cells, B cells, macrophages and myeloid dendritic cells were selected. The TIMER algorithm was applied for immune infiltration estimations. The estimated P-value was calculated via the purity-adjusted Spearman's rank correlation test to evaluate the associations between FGFs and infiltrating immune cells.

Establishment of a six-gene-based prognostic gene signature. Using the Cox regression model method, univariate and multivariate analyses were performed to determine whether the prognostic gene signature could be independent of other clinicopathological characteristics, including age, sex, pathological tumor-node-metastasis stage and tumor grade. $P < 0.05$ was considered to indicate a statistically significant difference. All independent prognostic factors determined by multivariate Cox regression analysis were included to build a nomogram to investigate the probability of 1-, 2-, 3- and 5-year OS of PAAD. All these analysis were perform with a web tool called ASSISTANT for Clinical Bioinformatics (https://www.aclbi.com/static/index.html#advance_prognosis).

IHC analysis. PAAD tissue chips (cat. no. PanA020PG03; Shanghai Xinchao Biological Technology Co., Ltd.) were fixed in 4% paraformaldehyde at room temperature for 48 h and embedded in paraffin with a section thickness of 5 μm . The tissue chips were successively placed in xylene for 10 min each, placed in absolute ethanol for 5 min, 75% alcohol for 5 min and washed with pure water. The tissue sections were placed in Tris-EDTA antigen repair buffer (pH9) in a microwave oven for antigen repair. The solution was heated at medium heat for 8 min and kept warm for 8 min before being transferred to medium and low heat for 7 min. After natural cooling, the glass slides were placed in PBS (pH7.2-7.4) and washed on a decolorization shaker 3 times, for 5 min each time. A total of 50 μl of 5-10% normal goat serum was added per chip for blocking (1:19 fold dilution) at room temperature for 30 min. Immunohistochemical staining of the paraffin-embedded tissues was performed using FGF2 (1:200; sc-74412; Santa Cruz Biotechnology, Inc.) and FGF8 (1:200; 20711-1-AP; ProteinTech Group, Inc.) primary antibodies, anti-mouse secondary antibodies (1:200; GB23301; Wuhan Servicebio Technology Co., Ltd.), anti-rabbit secondary antibodies (1:200; GB23303; Wuhan Servicebio Technology Co., Ltd.), and an ABC Elite immunoperoxidase kit (Wuhan Servicebio Technology Co., Ltd.) according to the manufacturer's instructions. Subsequently, all visual fields were observed under an optical microscope, and brown particles in the cell cytoplasm represented positive staining. IHC scoring was conducted according to the ratio and intensity of positive-staining areas. The staining areas were scored as follow: 0-15%, score 1; 16-50%, score 2; 51-100%, score 3.

The signal intensity was scored on a scale of 0-3: 0, negative; 1, weak; 2, moderate; and 3, strong. IHC scores were averaged from two experienced pathologists who scored the IHC staining independently. The IHC analysis involving human samples was approved by the West China Second University Hospital Institutional Review Board (Chengdu, China). All methods were performed in accordance with the relevant guidelines and regulations.

Cell culture and reagents. MIA Paca-2 cells (CL-0627) were purchased from Procell Life Science & Technology Co., Ltd., and maintained in DMEM (Gibco; Thermo Fisher Scientific, Inc.) supplemented with 10% FBS (Nanjing SenBeiJia Biological Technology Co., Ltd.) at 37°C in an incubator with 5% CO₂.

Cell colony formation assay. MIA Paca-2 cells were counted, plated in triplicate at a density of 800 cells per well in 6-well plates, and cultured in DMEM (supplemented with 10% FBS) at 37°C in an incubator with 5% CO₂. After 24 h, DMSO or 10 μM aloganib was used to treated the cells, and cultured for 6 days. Subsequently, the cells were washed twice with PBS and fixed in methanol for ~10 min at room temperature. After two additional washes with PBS, the cells were stained with crystal violet for 30 min at room temperature. Subsequently, the crystal violet was washed out, and the numbers of colonies (a mass of stained cells visible to the naked eye) were counted manually.

Statistical analysis. Statistical analysis was performed using R version 4.0.3 (<https://www.R-project.org>). Survival curves were plotted using the Kaplan-Meier method. For Kaplan-Meier curves, P-values were generated by log-rank tests or two-stage hazard rate comparison analyses, and hazard ratios (HRs) with 95% CIs was generated by univariate Cox proportional hazards regression. IHC data (tumor and paired adjacent tumor tissues) was analysed using Wilcoxon's signed rank test. All other comparisons were analyzed using an unpaired two-tailed Student's t test. $P < 0.05$ was considered to indicate a statistically significant difference.

Results

Associations among the FGF gene family. The FGF family is one of the most diverse growth factor groups in vertebrates. In humans, 22 FGF ligands have been identified, including FGF1, FGF2, FGF3, FGF4, FGF5, FGF6, FGF7, FGF8, FGF9, FGF10, FGF11, FGF12, FGF13, FGF14, FGF16, FGF17, FGF18, FGF19, FGF20, FGF21, FGF22 and FGF23 (25). According to bioinformatics analysis results, FGF6 and FGF23 cannot be detected in PAAD, so these two FGF members were not included in the present study. The potential interactions among the FGFs were examined by PPI network analysis. The details were as follows: Number of nodes, 22, number of edges, 124; average node degree, 11.3; and PPI enrichment, $P < 1.0 \times 10^{-16}$. These results indicated that there was a strong interaction among FGF family genes (Fig. 1A). Furthermore, the correlations between FGF family genes were also determined by analyzing their mRNA expression using the R software package ggstatsplot for PAAD, and Spearman's correlation analysis was included. The

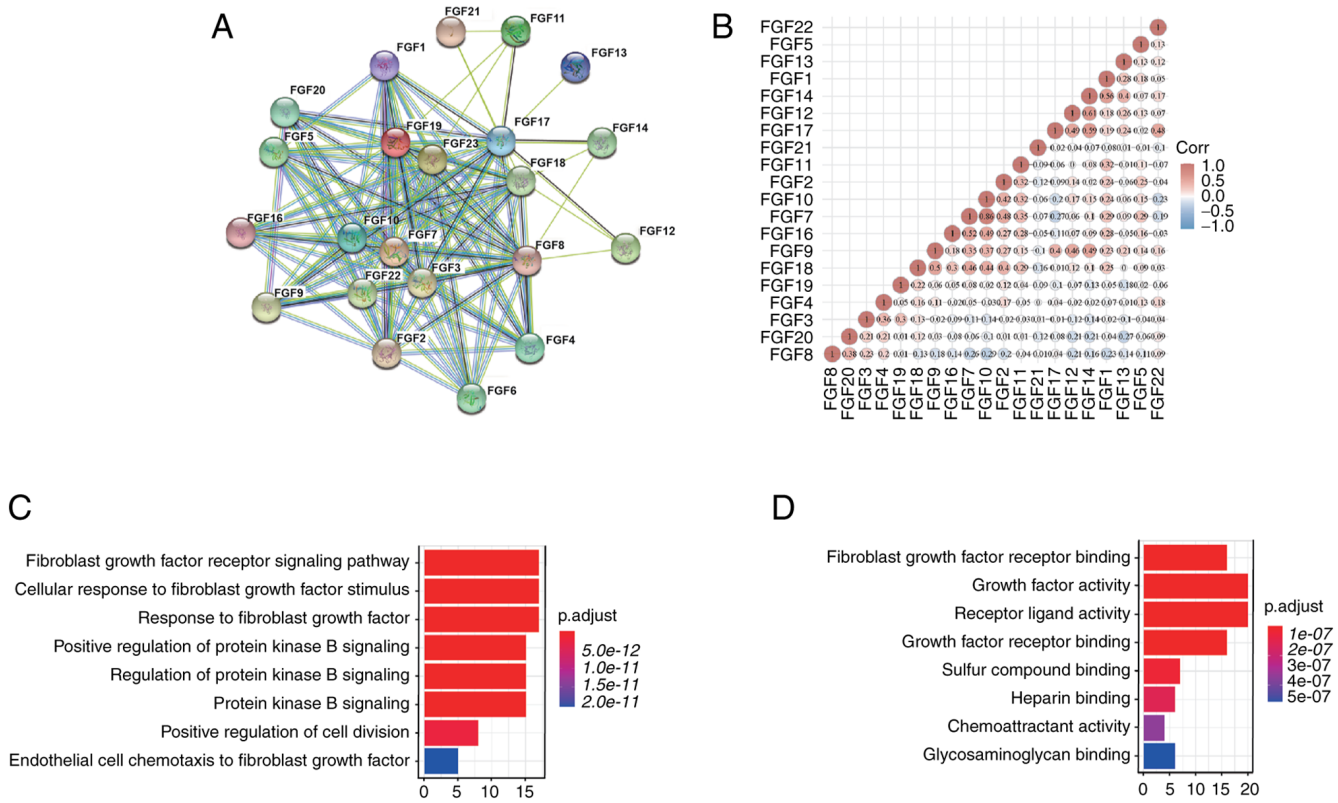


Figure 1. Related gene analysis and pathway function prediction of FGF gene family. (A) Protein-protein interaction network of the FGF gene family. (B) Correlation analysis of the FGF gene family. Functional enrichment analysis of the FGF gene family (C) biological processes and (D) molecular functions. Corr, correlation; FGF, fibroblast growth factor.

results showed significant positive correlations between genes such as FGF1 with FGF14, FGF12 with FGF14, and FGF7 with FGF16 and FGF10, among others (Fig. 1B). According to the functional enrichment analysis, FGF family genes were mainly associated with ‘fibroblast growth factor receptor signaling pathway’, ‘cellular response to fibroblast growth factor stimulus’, ‘response to fibroblast growth factor’ and ‘protein kinase B signaling’ (Fig. 1C). Furthermore, ‘growth factor activity’ and ‘receptor ligand activity’ were most frequently found for molecular functions (Fig. 1D).

Molecular subtype of PAAD based on FGF family genes. The Clusterplus package was used to perform consensus unsupervised clustering of 178 samples from patients with PAAD for FGF family genes, and the 178 PAAD samples are summarized in Table SI. The maximum number of clusters was 6 (Fig. 2A), and the cumulative distribution function curve of the FGF family genes indicated that k=3 appeared to be a suitable alternative for clustering (Fig. 2B). Additionally, the principal component analysis shown in Fig. 2C and consistency of the clustering results heatmap shown in Fig. 2D also indicated a relatively stable distribution of samples in the three clusters. Patients with PAAD were therefore divided into C1, C2 and C3 subtypes. A heatmap was drawn to show the gene expression of FGFs in the three subtypes (Fig. 2E). There was a significant difference among the C1 (n=108), C2 (n=61) and C3 (n=9) subtypes according to survival analysis (P=0.00071). The prognosis of the C3 subtype was significantly better than that of the C1 and C2 subtypes (Fig. 2F).

Construction and validation of the 6-gene signature. The LASSO regression method was utilized to identify the most significant prognostic genes among FGF family genes. The change trajectory of independent variables showed that the number of independent variable coefficients tending toward zero gradually increased with the gradual decrease in lambda. A risk model was built using the 10-fold cross-validation method, and the CI under each lambda was analyzed (Fig. 3A and B). The risk model of the six genes was as follows: Risk score = (0.1475)*FGF2 + (0.388)*FGF8 + (-0.1902)*FGF9 + (-0.0235)*FGF13 + (-0.5041)*FGF17 + (-0.4054)*FGF22.

The risk score of each patient with PAAD was computed, and the patients were assigned to the low-risk (n=89) or high-risk (n=89) group based on the median cut-off value. The distribution of the six genes across all samples revealed higher FGF2 expression in the patients in the high-risk group. By contrast, the patients in the low-risk group were likely to have higher FGF17 expression (Fig. 3C). The Kaplan-Meier analysis of all patients indicated that there was a significant difference between the low-risk and high-risk groups. The prognosis of the low-risk group was significantly better than that of the high-risk group. The median survival time of the high-risk group was 1.3 years and the median survival time of the low-risk group was 3.1 years (P=4.14x10⁻⁵; Fig. 3D). The area under the curve of the survival assessment model of the six genes was 0.684 at 1 year, 0.744 at 3 years and 0.819 at 5 years of OS (Fig. 3E).

Expression and prognostic value of the six FGF genes in PAAD. The mRNA expression levels of the six FGF genes

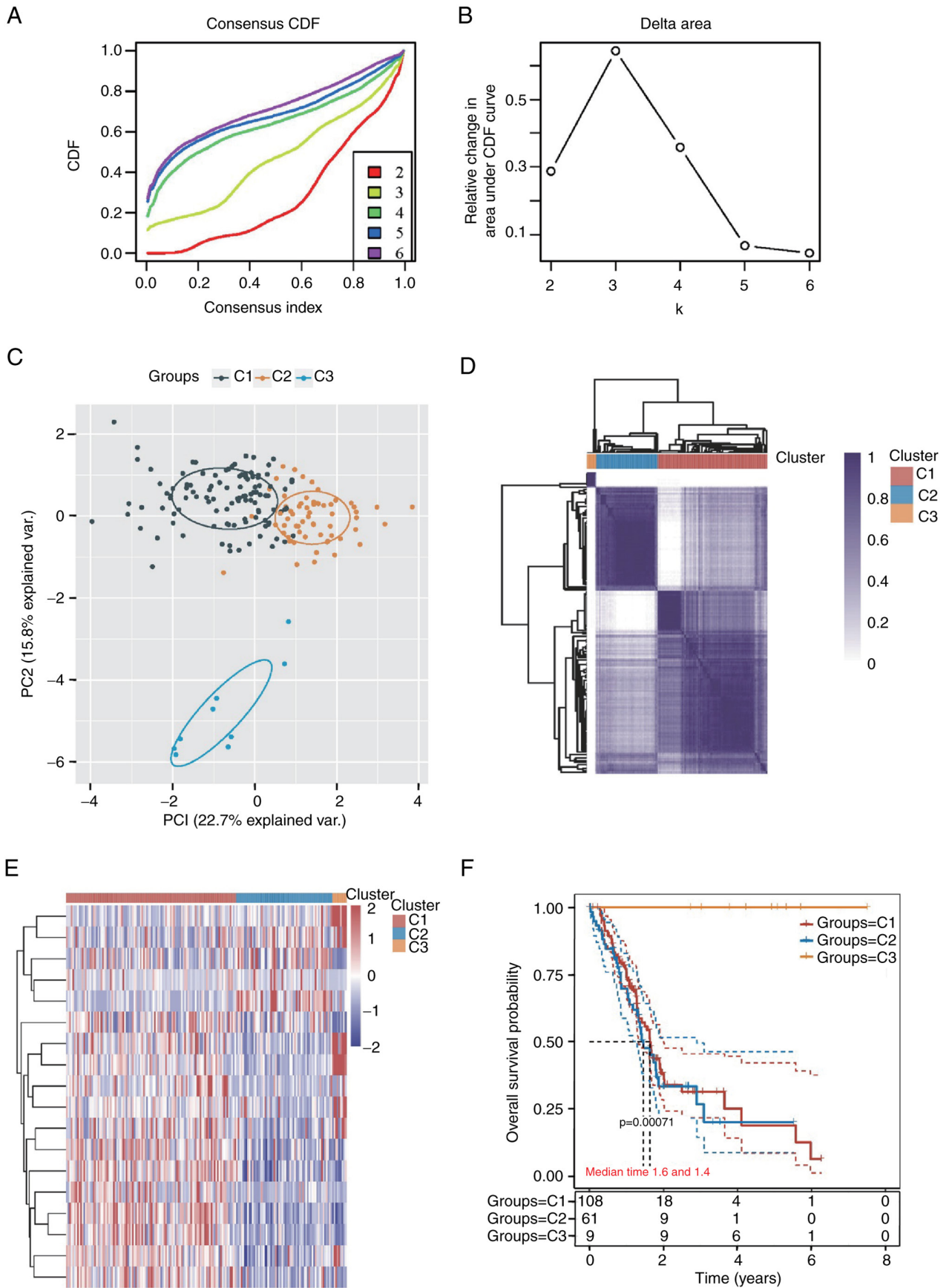


Figure 2. Molecular typing of pancreatic adenocarcinoma based on the fibroblast growth factor gene family. (A) CDF curve. Different colors represent different cluster numbers. (B) Delta area curve of consensus clustering. (C) Principal component analysis of the cluster groups (gene expression level varies from 0-1). (D) Heatmap of sample clustering at consensus k=3. (E) Gene expression heatmap of significant prognostic genes in three subtypes: C1, C2, C3. Red indicates high expression and blue indicates low expression (gene expression level varies from -2 to 2). (F) Survival curves of different cluster groups (C1 vs. C3, P<0.001; C3 vs. C2, P<0.001; C1 vs. C2, P=0.42; two-stage hazard rate comparison). CDF, cumulative distribution function; PC, principal component; %explained var., % explained value at risk.

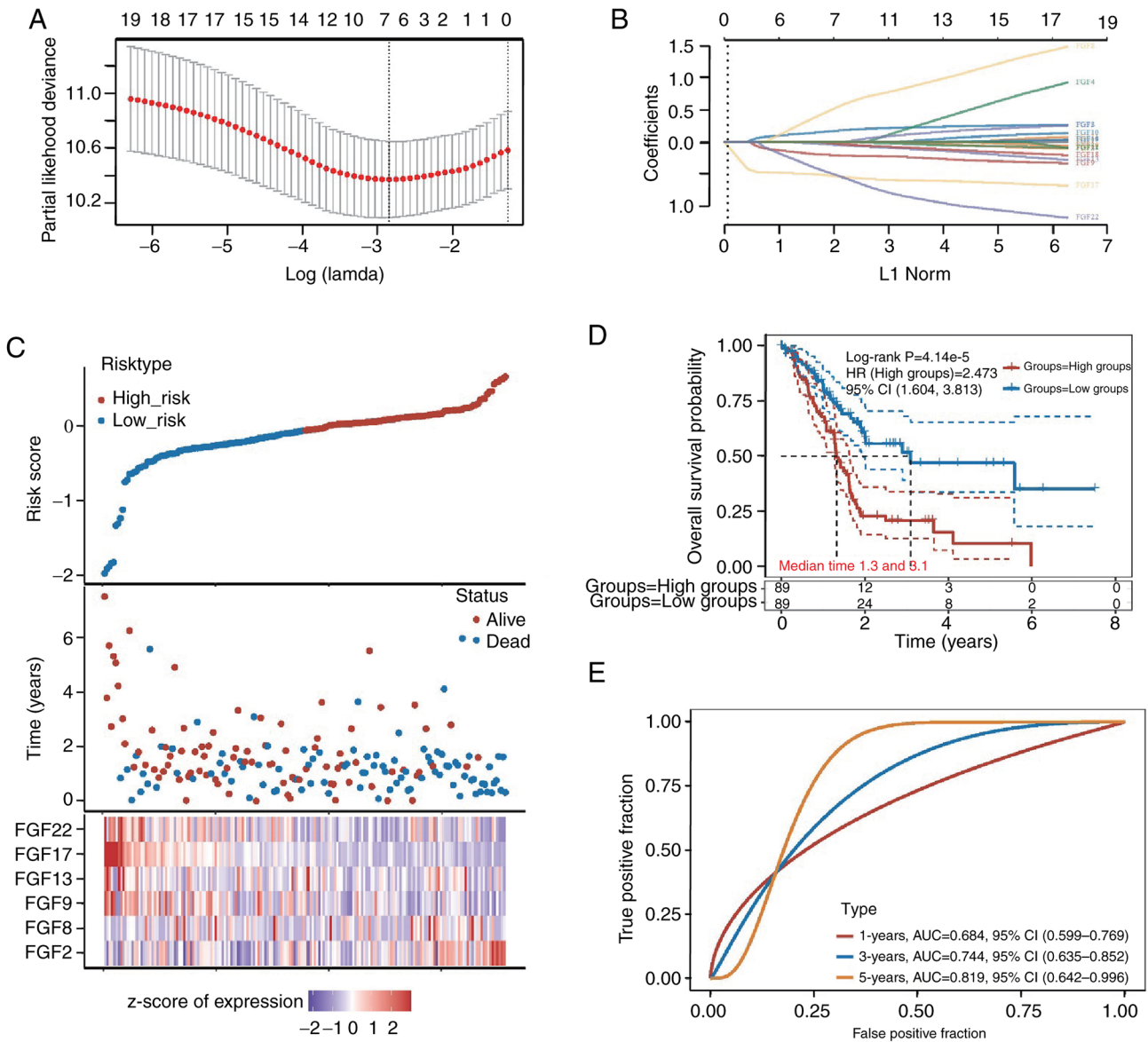


Figure 3. Construction and validation of the six-gene signature based on the FGF gene family. (A) The confidence interval under each λ . (B) The changing trajectory of each independent variable. The least absolute shrinkage and selection operator regression method was used to search for the hub genes. (C) Risk score distribution in the two groups, survival overview in the two groups and heatmap of the six genes in the two groups ($P=4.14 \times 10^{-5}$). (D) Survival curve of the two groups (Median time 1.3 and 9.1). (E) Time-dependent receiver operating characteristic curve for 1-, 3- and 5-year survival prediction. AUC, area under the curve; FGF, fibroblast growth factor; HR, hazard ratio.

were compared between pancreatic cancer tissues and normal pancreatic tissues using TCGA and GTEx data, and analyzed using GEPIA. The results demonstrated that the expression levels of FGF2 and FGF13 were higher in pancreatic cancer than in normal tissues (Fig. 4A-F). To further investigate the prognostic value of the six FGF genes in the survival of patients with PAAD, associations between the mRNA levels of the six FGF genes and clinical outcomes were analyzed using GEPIA. The Kaplan-Meier curve and two-stage hazard rate comparison analyses revealed that high transcriptional levels of FGF17 ($P=0.002$) and FGF22 ($P=0.002$) were significantly associated with long OS (Fig. 5A-F). These findings suggest that FGF22 and FGF17 may function as tumor suppressors in PAAD.

Associations of FGFs with tumor-infiltrating immune cells in patients with PAAD. Considering the significant roles

of immune cell infiltration in the tumor microenvironment (TME), the present study investigated the relationships between the 6 FGFs and immune cell infiltration based on the TIMER database. FGF2 expression was positively associated with infiltration of CD8⁺ T cells, B cells, macrophages and myeloid dendritic cells in patients with PAAD (Fig. 6A). FGF8 expression was negatively correlated with the infiltration of CD8⁺ T cells, macrophages and myeloid dendritic cells (Fig. 6B). Additionally, there was a positive correlation between FGF9 expression and infiltration of CD8⁺ T cells, CD4⁺ T cells, macrophages and myeloid dendritic cells (Fig. 6C). FGF13 expression was positively associated with infiltration of CD8⁺ T cells, macrophages and myeloid dendritic cells (Fig. 6D). Regarding FGF17, there was a negative correlation between infiltration of CD8⁺ T cells and myeloid dendritic cells and FGF17 expression, while CD4⁺ T

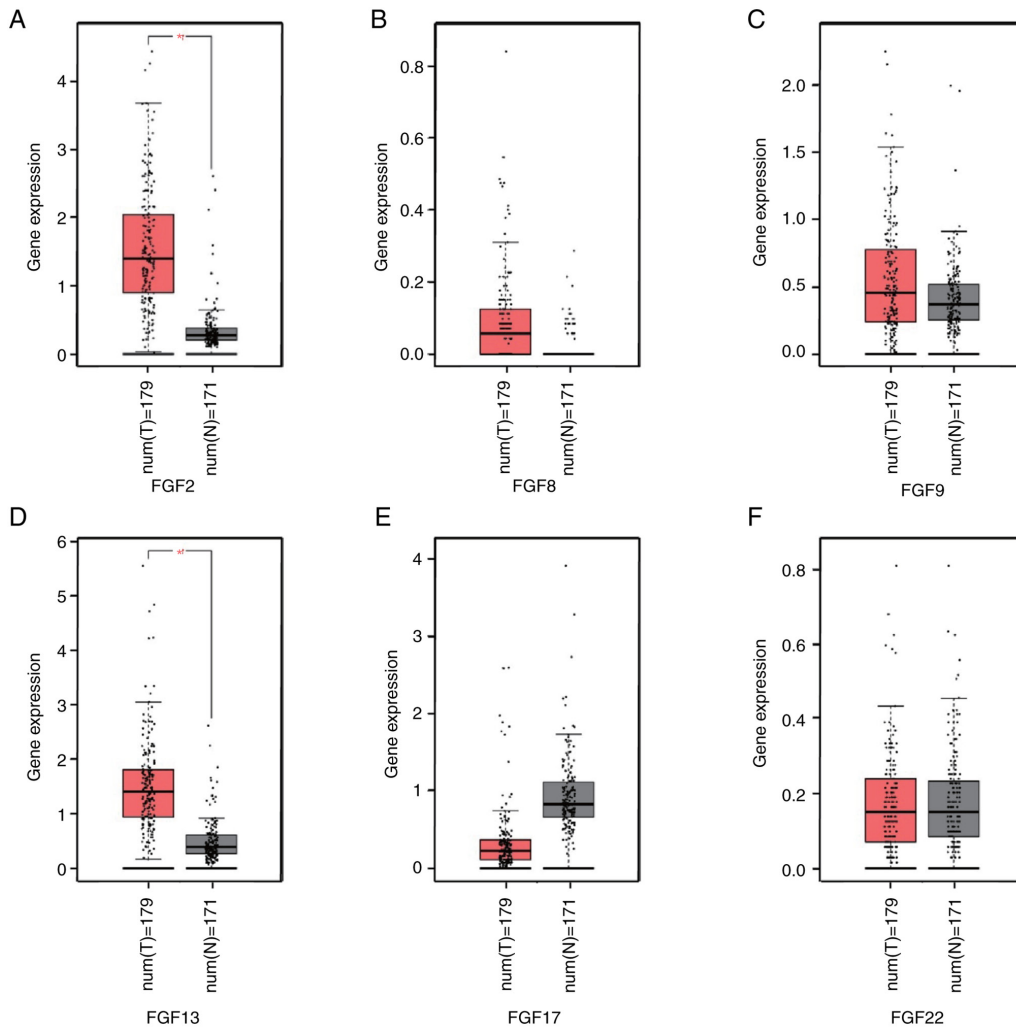


Figure 4. Expression of FGFs in PAAD (Gene Expression Profiling Interactive Analysis). Expression of (A) FGF2, (B) FGF8, (C) FGF9, (D) FGF13, (E) FGF17 and (F) FGF22 in PAAD. *P<0.05. FGF, fibroblast growth factor; PAAD, pancreatic adenocarcinoma; N, normal tissues; T, tumor tissues.

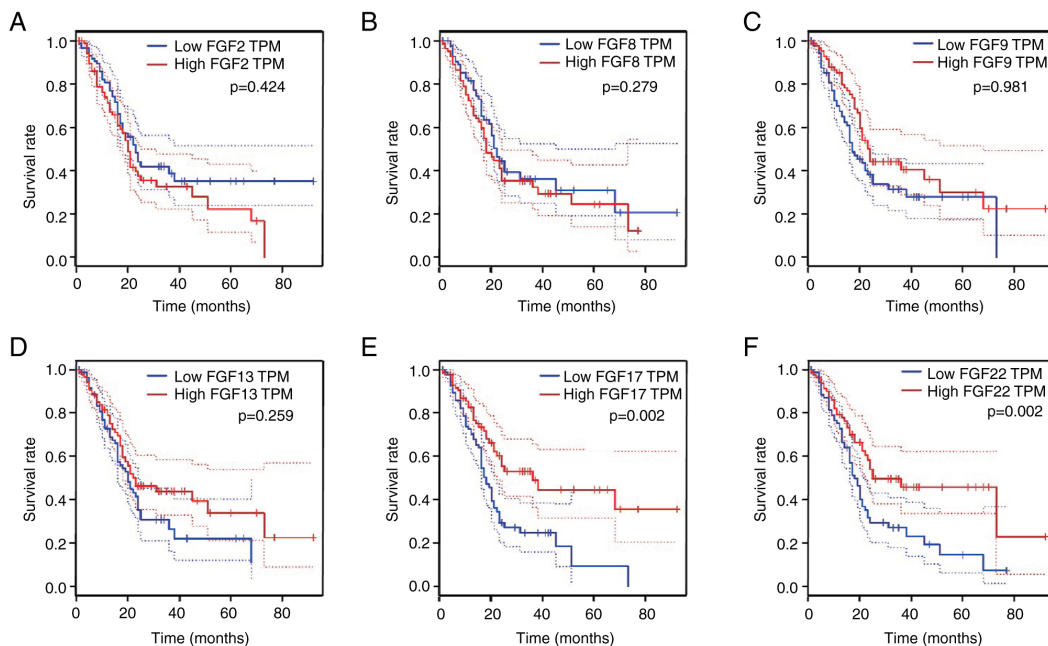


Figure 5. Prognostic value of FGFs in PAAD (Gene Expression Profiling Interactive Analysis). Prognostic value of the mRNA expression of (A) FGF2, (B) FGF8, (C) FGF9, (D) FGF13, (E) FGF17 and (F) FGF22 in PAAD. FGF, fibroblast growth factor; PAAD, pancreatic adenocarcinoma; TPM, transcripts per million.

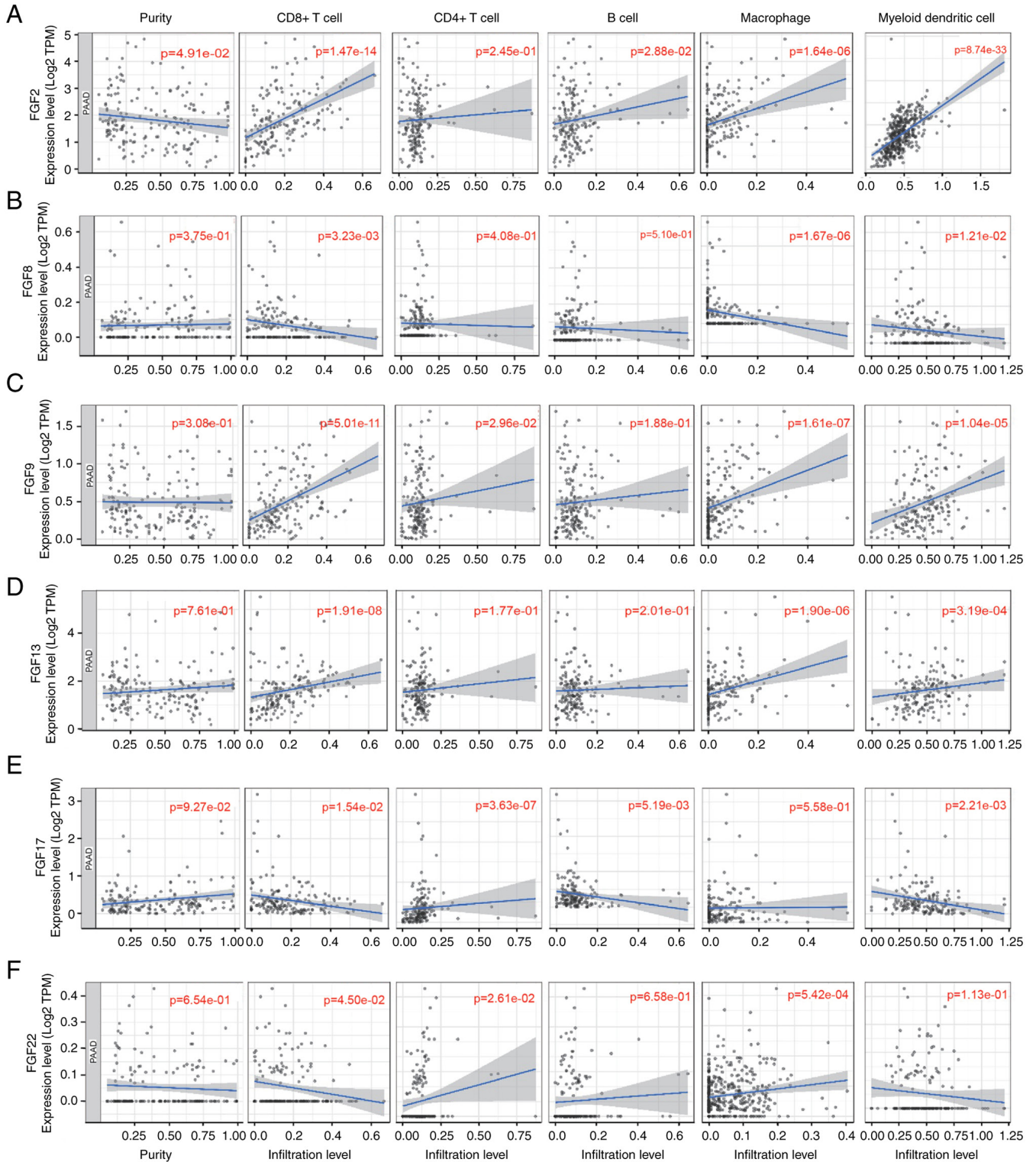


Figure 6. Correlations between differentially expressed FGFs and immune cell infiltration (Tumor Immune Estimation Resource). Correlations between the abundance of immune cells and the expression of (A) FGF2, (B) FGF8, (C) FGF9, (D) FGF13, (E) FGF17 and (F) FGF22. FGF, fibroblast growth factor; PAAD, pancreatic adenocarcinoma; TPM, transcripts per million.

cells were positively associated with FGF17 (Fig. 6E). FGF22 expression was shown to have a positive correlation with the infiltration of CD4⁺ T cells and macrophages, but a negative correlation with the infiltration of CD8⁺ T cells (Fig. 6F).

Construction and validation of a two-gene signature in patients with PAAD. Subsequently, the present study

explored the prognostic role of FGF family genes in PAAD. Six genes, FGF2, FGF8, FGF9, FGF13, FGF17 and FGF22, were identified by univariate Cox regression analysis in TCGA-PAAD datasets. The results demonstrated that FGF2, FGF17, FGF9, FGF22 and FGF13 were significantly associated with the prognosis of PAAD. As shown in forest maps, of all the factors, FGF2 (HR=1.28211; P=0.00690), FGF17

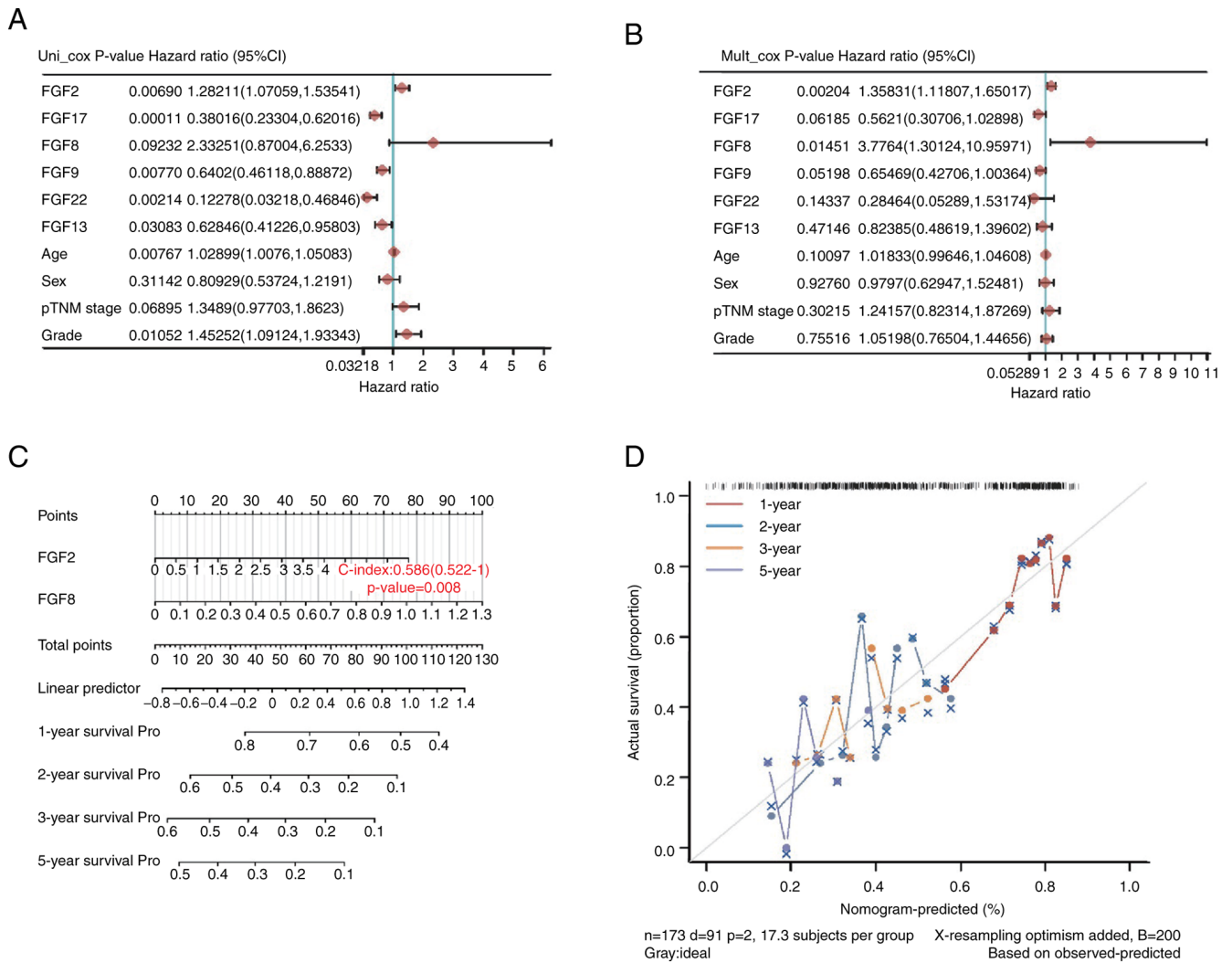


Figure 7. Clinical diagnostic value of the six-gene signature. (A) Univariate Cox analysis of FGF genes in the TCGA-PAAD cohort. (B) Multivariate Cox analysis of FGF genes in the TCGA-PAAD cohort. (C) Nomogram for predicting the 1-, 2-, 3- and 5-year overall survival of patients. (D) The 1-, 2-, 3- and 5-year calibration curves of the nomogram. FGF, fibroblast growth factor; PAAD, pancreatic adenocarcinoma; Pro, probability; TCGA, The Cancer Genome Atlas.

(HR=0.38016; P=0.00011), FGF9 (HR=0.6402; P=0.00770), FGF22 (HR=0.12278; P=0.00214) and FGF13 (HR=0.62846; P=0.03083) were significantly associated with the survival of patients with PAAD (Fig. 7A). To reveal the independent prognostic factors in patients with PAAD, the six genes and other clinical variables were further analyzed using multivariate Cox regression analyses. FGF2 (HR=1.35831; P=0.00204) and FGF8 (HR=3.7764; P=0.01451) were independent risk factors for the prognosis of patients with PAAD (Fig. 7B).

A nomogram was constructed with FGF2 and FGF8. The C-index of this model was 0.586 (P=0.008), suggesting that the risk model based on FGF2 and FGF8 had good performance in predicting the prognosis of PAAD (Fig. 7C). According to the 1-, 2-, 3- and 5-year nomograms, the predicted survival rate was close to the actual survival outcome (Fig. 7D). Furthermore, IHC was performed to test FGF2 and FGF8 protein expression in PAAD cancer tissues and paired adjacent tissues. FGF2 and FGF8 were more highly expressed in PAAD cancer tissues than in paired adjacent tissues (Fig. 8A-C). These results indicated that the two-gene signature constructed by FGF2 and FGF8 is helpful to predict the development of PAAD.

FGFs are heparin-binding polypeptides, the majority of which are secreted ligands that communicate via four transmembrane FGF receptors (FGFRs) with great affinity. Alofanib is an allosteric inhibitor of FGFR2 (26). To evaluate the impact of FGFRs on PAAD, MIA Paca-2 cells were treated with 10 μM alofanib. The colony formation of MIA Paca-2 cells was decreased following alofanib treatment (P<0.05; Fig. 8D and E).

Discussion

PAAD is a highly malignant tumor with a poor prognosis and a 5-year survival rate of <5%, and its morbidity has steadily increased worldwide over the past 3 decades (27). It has previously been reported that pancreatic cancer is divided into several molecular subgroups, each with its own set of biological characteristics, which contributes to the lack of efficacy and drug resistance observed for current treatments (28). Systematic genomic analysis has revealed four key driver genes in pancreatic cancer: KRAS, cyclin dependent kinase inhibitor 2A, TP53 and SMAD4 (29,30). At present,

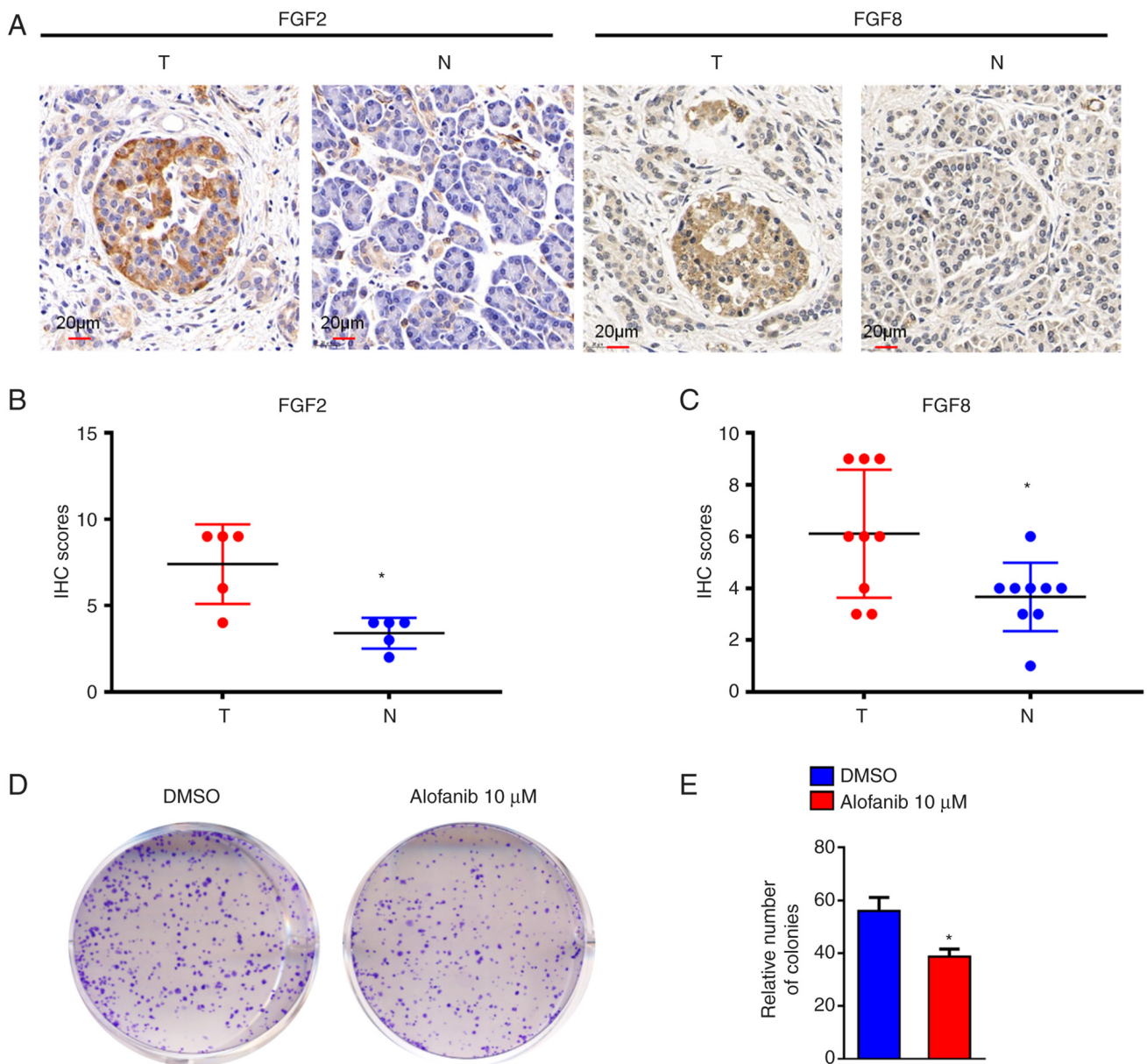


Figure 8. Expression and influence of FGF2 and FGF8 in pancreatic adenocarcinoma. (A) Expression of FGF2 and FGF8 in pancreatic adenocarcinoma. Scale bar, 20 μm . Quantification analysis of IHC for (B) FGF2 ($P=0.0313$; Wilcoxon's signed rank test) and (C) FGF8 ($P=0.0391$; Wilcoxon's signed rank test) ($^*P<0.05$). (D) Colony formation assay using MIA Paca-2 cells treated with DMSO or 10 μM alofanib for 7 days. (E) Colony numbers are presented as the mean \pm SD ($n=3$). $^*P<0.05$. Unpaired Student's t-test. FGF, fibroblast growth factor; IHC, immunohistochemistry; N, normal tissue; T, tumor tissue.

there is no effective clinical treatment for PAAD that targets these genes. Significant clinical improvements in diagnostic investigations, surgical procedures and systemic medicines should enhance pancreatic cancer outcomes. An improved understanding of pancreatic cancer biology and genetics, including novel information on driver gene alterations, tumor metabolism and the TME, might contribute to attractive and creative effective treatments (31). Immunotherapy has become increasingly utilized in the treatment of PAAD (32). Despite the overwhelming success of immune checkpoint inhibitors in leukemia and melanoma, PAAD is an outlier due to its immunosuppressive TME and poor tumor immunogenicity (33).

The TME is becoming an increasingly important research area and may affect tumor progression and recurrence (34,35). Immune cells in the TME are reportedly involved in inhibiting or promoting tumor activity and are critical factors in determining

clinical outcomes and immunotherapy efficacy (36). PAAD is characterized by extensive desmoplasia in the TME (37). The interaction between PAAD cells and the TME is the most important driving force of desmoplasia. Increasing evidence indicates that the TME actively contributes to tumor growth and metastasis (38). Therefore, FGFs, which serve as parts of the TME, may be involved in the occurrence and development of PAAD. Although FGFs serve key roles in head and neck squamous cell carcinomas (39) and hepatocellular carcinoma (40,41), the distinct roles of FGFs in PAAD remain to be elucidated. We hypothesized that FGFs also serve a critical role in predicting the prognosis of patients with PAAD. A composed model constructed with various relevant genes is a better choice to predict prognosis compared with a single gene (42). Therefore, in the present study, the FGF gene family in PAAD was analyzed systematically regarding expression, prognostic value and immune cell infiltration.

According to the bioinformatics analysis, a prognostic signature based on 6 FGFs (FGF2, FGF8, FGF9, FGF13, FGF17 and FGF22) was constructed, which performed appropriately in prognostic predictions in patients with PAAD. Patients in the high-risk group had shorter survival times than those in the low-risk group. Furthermore, the TCGA-PAAD cohort was used to analyze the six genes by univariate and multivariate Cox regression analyses. The results demonstrated that FGF2 and FGF8 were significantly associated with survival and were independent risk factors for the prognosis of patients with PAAD. The IHC results demonstrated that the expression of the two genes was elevated in PAAD cancer tissues compared with in normal tissues. These results indicated that FGF2 and FGF8 function as oncogenes and might serve an important role in the tumorigenesis and progression of PAAD. FGF2 is reportedly involved in the occurrence and development of various cancer types, such as NSCLC (43) and osteosarcoma (44). Furthermore, FGF2 has been reported to serve an important role in the treatment of oncolytic viruses in PAAD (45). FGF8 also deserves attention in numerous types of malignancies (46,47). FGF8 is upregulated in patients with oral squamous cell carcinoma, and high FGF8 expression is related to a set of clinicopathologic parameters, including age, drinking and survival time (48). The aforementioned conclusions demonstrated that FGF2 and FGF8 have potential as cell markers for tumors. In the present study, high FGF2 and FGF8 mRNA expression was significantly associated with short OS time in patients with PAAD. These results illustrate that FGF2 and FGF8 serve oncogenic roles in PAAD. Furthermore, a nomogram was constructed based on FGF2 and FGF8. The calibration map showed that the present model had a good ability to predict the prognosis of patients with PAAD.

Acknowledgements

Not applicable.

Funding

The present study was supported by the West China Second University Hospital Clinical Research Fund (grant no. KL105), the Sichuan Provincial Key Research and Development Projects (grant no. 2022YFS0242), the West China Second University Hospital Clinical Discipline Development Fund (grant no. KL066) and Cadres Healthcare Research Projects in Sichuan Province (grant no. 2021-1703).

Availability of data and materials

The datasets analyzed during the current study are available in the Cancer Genome Atlas (TCGA, <http://can-cernome.nih.gov/>), Assistant for Clinical Bioinformatics (<https://www.aclbi.com/static/index.html#/>) and TIMER (<http://timer.cistrome.org/>) databases. All other datasets used and/or analyzed during the current study are available from the corresponding author on reasonable request.

Authors' contributions

YXC wrote the manuscript. JM, XJL and YMJ designed and supervised the implementation of the entire study. LY and JJH

analyzed the data and completed the immunohistochemistry experiment. YXC analyzed the data and completed the cell colony formation assay. XJL and YMJ provided professional opinions on the research and revised the manuscript. YXC and JM confirm the authenticity of all the raw data. All authors read and approved the final manuscript.

Ethics approval and consent to participate

All experiments involving human samples were approved by the West China Second University Hospital Institutional Review Board (Chengdu, China).

Patient consent for publication

Not applicable.

Competing interests

The authors declare that they have no competing interests.

References

- Sung H, Ferlay J, Siegel RL, Laversanne M, Soerjomataram I, Jemal A and Bray F: Global cancer statistics 2020: GLOBOCAN estimates of incidence and mortality worldwide for 36 cancers in 185 countries. *CA Cancer J Clin* 71: 209-249, 2021.
- Siegel RL, Miller KD and Jemal A: Cancer statistics, 2019. *CA Cancer J Clin* 69: 7-34, 2019.
- Fukushima G, Abe K, Kitago M, Iwasaki E, Hirata A, Takemura R, Ishii R, Yagi H, Abe Y, Hasegawa Y, *et al*: Association between clinical backgrounds and malignant progression of suspected intraductal papillary mucinous neoplasm. *Pancreas* 51: 617-623, 2022.
- Brugel M, Carlier C, Reyes-Castellanos G, Callon S, Carrier A and Bouche O: Pesticides and pancreatic adenocarcinoma: A transversal epidemiological, environmental and mechanistic narrative review. *Dig Liver Dis* 8: S1590-S8658, 2022.
- Okita Y, Sobue T, Zha L, Kitamura T, Iwasaki M, Inoue M, Yamaji T, Tsugane S and Sawada N: Association between alcohol consumption and risk of pancreatic cancer: The Japan public health center-based prospective study. *Cancer Epidemiol Biomark Prev* 3: EPI-22-0216, 2022.
- Irisawa A, Takeno M, Watanabe K, Takahashi H, Mitsunaga S and Ikeda M: Incidence of and risk factors for severe neutropenia during treatment with the modified FOLFIRINOX therapy in patients with advanced pancreatic cancer. *Sci Rep* 12: 15574, 2022.
- Molinelli S, Vai A, Russo S, Loap P, Meschini G, Paganelli C, Barcellini A, Vitolo V, Orlandi E and Ciocca M: The role of multiple anatomical scenarios in plan optimization for carbon ion radiotherapy of pancreatic cancer. *Radiother Oncol* 176: 1-8, 2022.
- Alshemry AK, Alsaleh NB, Alkhudair N, Alzhrani R and Alshamsan A: Recent nanotechnology advancements to treat multidrug-resistance pancreatic cancer: Pre-clinical and clinical overview. *Front Pharmacol* 13: 933457, 2022.
- Gautam SK, Basu S, Aithal A, Dwivedi NV, Gulati M and Jain M: Regulation of pancreatic cancer therapy resistance by chemokines. *Semin Cancer Biol* 86: 69-80, 2022.
- Kang X, Lin Z, Xu M, Pan J and Wang ZW: Deciphering role of FGF/R signalling pathway in pancreatic cancer. *Cell Prolif* 52: e12605, 2019.
- Thomas D and Radhakrishnan P: Tumor-stromal crosstalk in pancreatic cancer and tissue fibrosis. *Mol Cancer* 18: 14, 2019.
- Zhang Z, Qin Y, Ji S, Xu W, Liu M, Hu Q, Ye Z, Fan G, Yu X, Liu W and Xu X: FGF/BP1-mediated crosstalk between fibroblasts and pancreatic cancer cells via FGF22/FGFR2 promotes invasion and metastasis of pancreatic cancer. *Acta Biochim Biophys Sin(Shanghai)* 53: 997-1008, 2021.
- El-Hariry I, Pignatelli M and Lemoine NR: FGF-1 and FGF-2 regulate the expression of E-cadherin and catenins in pancreatic adenocarcinoma. *Int J Cancer* 94: 652-661, 2001.

14. Pecqueux C, Arslan A, Heller M, Falkenstein M, Kaczorowski A, Tolstov Y, Sülthmann H, Grüllich C, Herpel E, Duensing A, *et al*: FGF-2 is a driving force for chromosomal instability and a stromal factor associated with adverse clinico-pathological features in prostate cancer. *Urol Oncol* 36: 365 e315-365 e326, 2018.
15. Sun C, Tian X, Jia Y, Yang M, Li Y and Fernig DG: Functions of exogenous FGF signals in regulation of fibroblast to myofibroblast differentiation and extracellular matrix protein expression. *Open Biol* 12: 210356, 2022.
16. Belov AA and Mohammadi M: Molecular mechanisms of fibroblast growth factor signaling in physiology and pathology. *Cold Spring Harb Perspect Biol* 5: a015958, 2013.
17. Bock FJ, Sedov E, Koren E, Koessinger AL, Cloix C, Zerbst D, Athineos D, Anand J, Campbell KJ, Blyth K, *et al*: Apoptotic stress-induced FGF signalling promotes non-cell autonomous resistance to cell death. *Nat Commun* 12: 6572, 2021.
18. Guo K, Ma Z, Zhang Y, Han L, Shao C, Feng Y, Gao F, Di S, Zhang Z, Zhang J, *et al*: HDAC7 promotes NSCLC proliferation and metastasis via stabilization by deubiquitinase USP10 and activation of beta-catenin-FGF18 pathway. *J Exp Clin Cancer Res* 41: 91, 2022.
19. Xu Z, Cai Y, Liu W, Kang F, He Q, Hong Q, Zhang W, Li J, Yan Y and Peng J: Downregulated exosome-associated gene FGF9 as a novel diagnostic and prognostic target for ovarian cancer and its underlying roles in immune regulation. *Aging (Albany NY)* 14: 1822-1835, 2022.
20. Carter EP, Coetzee AS, Bort ET, Wang Q, Kocher HM and Grose RP: Dissecting FGF signalling to target cellular crosstalk in pancreatic cancer. *Cells* 10: 847, 2021.
21. Peng J, Sridhar S, Siefker-Radtke AO, Selvarajah S and Jiang DM: Targeting the FGFR pathway in urothelial carcinoma: The future is now. *Curr Treat Options Oncol* 23: 1269-1287, 2022.
22. Ohtsu A, Arai S, Sawada T, Kato M, Maeno Y, Miyazawa Y, Fujizuka Y, Sekine Y, Koike H, Matsui H and Suzuki K: Fibroblast growth factor receptor inhibitor erdafitinib promotes Mcl-1 degradation and synergistically induces apoptosis with Bcl-xL/Bcl-2 inhibitor in urothelial cancer cells. *Biochem Biophys Res Commun* 628: 76-83, 2022.
23. Wu Y, Yi Z, Li J, Wei Y, Feng R, Liu J, Huang J, Chen Y, Wang X, Sun J, *et al*: FGFR blockade boosts T cell infiltration into triple-negative breast cancer by regulating cancer-associated fibroblasts. *Theranostics* 12: 4564-4580, 2022.
24. Karajannis MA, Vincent L, Drenzo R, Shmelkov SV, Zhang F, Feldman EJ, Bohlen P, Zhu Z, Sun H, Kussie P and Rafii S: Activation of FGFR1beta signaling pathway promotes survival, migration and resistance to chemotherapy in acute myeloid leukemia cells. *Leukemia* 20: 979-986, 2006.
25. Xie Y, Su N, Yang J, Tan Q, Huang S, Jin M, Ni Z, Zhang B, Zhang D, Luo F, *et al*: FGF/FGFR signaling in health and disease. *Signal Transduct Target Ther* 5: 181, 2020.
26. Tyulyandina A, Harrison D, Yin W, Stepanova E, Kochenkov D, Solomko E, Peretolchina N, Daeyaert F, Joos JB, Aken KV, *et al*: Alofanib, an allosteric FGFR2 inhibitor, has potent effects on ovarian cancer growth in preclinical studies. *Invest New Drugs* 35: 127-133, 2017.
27. Gillen S, Schuster T, Büschenfelde CM, Friess H and Kleeff J: Preoperative/neoadjuvant therapy in pancreatic cancer: A systematic review and meta-analysis of response and resection percentages. *PLoS Med* 7: e1000267, 2010.
28. Zhu H, Wei M, Xu J, Hua J, Liang C, Meng Q, Zhang Y, Liu J, Zhang B, Yu X and Shi S: PARP inhibitors in pancreatic cancer: Molecular mechanisms and clinical applications. *Mol Cancer* 19: 49, 2020.
29. Biankin AV, Waddell N, Kassahn KS, Gingras MC, Muthuswamy LB, Johns AL, Miller DK, Wilson PJ, Patch AM, Wu J, *et al*: Pancreatic cancer genomes reveal aberrations in axon guidance pathway genes. *Nature* 491: 399-405, 2012.
30. Singhi AD, George B, Greenbowe JR, Chung J, Suh J, Maitra A, Klempner SJ, Hendifar A, Milind JM, Golan T, *et al*: Real-time targeted genome profile analysis of pancreatic ductal adenocarcinomas identifies genetic alterations that might be targeted with existing drugs or used as biomarkers. *Gastroenterology* 156: 2242-2253.e2244, 2019.
31. Wang S, Zheng Y, Yang F, Zhu L, Zhu XQ, Wang ZF, Wu XL, Zhou CH, Yan JY, Hu BY, *et al*: The molecular biology of pancreatic adenocarcinoma: Translational challenges and clinical perspectives. *Signal Transduct Target Ther* 6: 249, 2021.
32. Luong T, Golivi Y, Nagaraju GP and El-Rayes BF: Fibroblast heterogeneity in pancreatic ductal adenocarcinoma: Perspectives in immunotherapy. *Cytokine Growth Factor Rev* 8: S1359-S6101, 2022.
33. Zhou W, Zhou Y, Chen X, Ning T, Chen H, Guo Q, Zhang Y, Liu P, Zhang Y, Li C, *et al*: Pancreatic cancer-targeting exosomes for enhancing immunotherapy and reprogramming tumor microenvironment. *Biomaterials* 268: 120546, 2021.
34. Quail DF and Joyce JA: Microenvironmental regulation of tumor progression and metastasis. *Nat Med* 19: 1423-1437, 2013.
35. Deepak KGK, Vempati R, Nagaraju GP, Dasari VR, Nagini S, Rao DN and Malla RR: Tumor microenvironment: Challenges and opportunities in targeting metastasis of triple negative breast cancer. *Pharmacol Res* 153: 104683, 2020.
36. Devlin MJ, Miller R, Laforets F, Kotantaki P, Garsed DW, Kristeleit R, Bowtell DD, McDermott J, Maniati E and Balkwill FR: The tumour microenvironment of clear cell ovarian cancer. *Cancer Immunol Res* 12: CIR-202-0407, 2022.
37. Ren B, Cui M, Yang G, Wang H, Feng M, You L and Zhao Y: Tumor microenvironment participates in metastasis of pancreatic cancer. *Mol Cancer* 17: 108, 2018.
38. Rubin SJS, Sojwal RS, Gubatan J and Rogalla S: The tumor immune microenvironment in pancreatic ductal adenocarcinoma: Neither hot nor cold. *Cancers (Basel)* 14: 4236, 2022.
39. Bao Y, Gabrielpillai J, Dietrich J, Zarbl R, Strieth S, Schröck F and Dietrich D: Fibroblast growth factor (FGF), FGF receptor (FGFR), and cyclin D1 (CCND1) DNA methylation in head and neck squamous cell carcinomas is associated with transcriptional activity, gene amplification, human papillomavirus (HPV) status, and sensitivity to tyrosine kinase inhibitors. *Clin Epigenetics* 13: 228, 2021.
40. Raja A, Park I, Haq F and Ahn SM: FGF19-FGFR4 signaling in hepatocellular carcinoma. *Cells* 8: 536, 2019.
41. Tovar V, Cornella H, Moeini A, Vidal S, Hoshida Y, Sia D, Peix J, Cabellos L, Alsinet C, Torrecilla S, *et al*: Tumour initiating cells and IGF/FGF signalling contribute to sorafenib resistance in hepatocellular carcinoma. *Gut* 66: 530-540, 2017.
42. Zhu Z, Tang C, Xu T and Zhao Z: Molecular analysis of prognosis and immune pathways of pancreatic cancer based on TNF family members. *J Oncol* 2021: 2676996, 2021.
43. Wang J, Shu H and Guo S: MiR-646 suppresses proliferation and metastasis of non-small cell lung cancer by repressing FGF2 and CCND2. *Cancer Med* 9: 4360-4370, 2020.
44. Yang B, Li L, Tong G, Zeng Z, Tan J, Su Z, Liu Z, Lin J, Gao W, Chen J, *et al*: Circular RNA circ_001422 promotes the progression and metastasis of osteosarcoma via the miR-195-5p/FGF2/PI3K/Akt axis. *J Exp Clin Cancer Res* 40: 235, 2021.
45. Ilkow CS, Marguerie M, Batenchuk C, Mayer J, Neriah DB, Cousineau S, Falls T, Jennings VA, Boileau M, Bellamy D, *et al*: Reciprocal cellular cross-talk within the tumor microenvironment promotes oncolytic virus activity. *Nat Med* 21: 530-536, 2015.
46. Wilmerding A, Bouteille L, Caruso N, Bidaut G, Etchevers HC, Graba Y and Delfini MC: Sustained experimental activation of FGF8/ERK in the developing chicken spinal cord models early events in ERK-mediated tumorigenesis. *Neoplasia* 24: 120-132, 2022.
47. Jomrich G, Hudec X, Harpain F, Winkler D, Timelthaler G, Mohr T, Marian B and Schoppmann SF: Expression of FGF8, FGF18, and FGFR4 in gastroesophageal adenocarcinomas. *Cells* 8: 1092, 2019.
48. Hao Y, Xiao Y, Liao X, Tang S, Xie X, Liu R and Chen Q: FGF8 induces epithelial-mesenchymal transition and promotes metastasis in oral squamous cell carcinoma. *Int J Oral Sci* 13: 6, 2021.



This work is licensed under a Creative Commons Attribution-NonCommercial-NoDerivatives 4.0 International (CC BY-NC-ND 4.0) License.